

PAPER • OPEN ACCESS

## Validation of wind turbine wake models with focus on the dynamic wake meandering model

To cite this article: I. Reinhardt *et al* 2018 *J. Phys.: Conf. Ser.* **1037** 072028

View the [article online](#) for updates and enhancements.

### Related content

- [Validation of the Dynamic Wake Meander model with focus on tower loads](#)  
T.J. Larsen, G.C. Larsen, M.M. Pedersen *et al.*
- [Reduced order model of the inherent turbulence of wind turbine wakes inside an infinitely long row of turbines](#)  
S J Andersen, J N Sørensen and R Mikkelsen
- [An annual energy production estimation methodology for onshore wind farms over complex terrain using a RANS model with actuator discs](#)  
Gonzalo P. Navarro Diaz, Matias Avila and Arnau Folch



**IOP | ebooks™**

Bringing you innovative digital publishing with leading voices to create your essential collection of books in STEM research.

Start exploring the collection - download the first chapter of every title for free.

# Validation of wind turbine wake models with focus on the dynamic wake meandering model

I. Reinwardt<sup>1</sup>, N. Gerke<sup>1</sup>, P. Dalhoff<sup>2</sup>, D. Steudel<sup>3</sup>, W. Moser<sup>4</sup>

<sup>1</sup> Research assistant, Hamburg University of Applied Sciences, Hamburg, GER

<sup>2</sup> Professor, Hamburg University of Applied Sciences, Hamburg, GER

<sup>3</sup> Expert Engineer, Nordex Energy GmbH, Hamburg, GER

<sup>4</sup> Senior Expert Engineer, Nordex Energy GmbH, Hamburg, GER

E-mail: [inga.reinwardt@haw-hamburg.de](mailto:inga.reinwardt@haw-hamburg.de)

**Abstract.** This analysis compares current wake models, such as the Sten Frandsen turbulence model, an engineering wind speed deficit and turbulence model developed by G. Chr. Larsen, the N. O. Jensen wind speed deficit description and three variations of the dynamic wake meandering (DWM) model to measurements from onshore wind farms. Special attention is given to the dynamic wake meandering model. Today different versions or implementations of the dynamic wake meandering model exist. These versions differ among others in the calculation of the quasi-steady wake deficit in the meandering frame of reference. The influence of these calculation methods on loads and yield is analysed in this work. The validation of the mentioned wake models is based on turbine load, power and wind measurements from two onshore wind farms. One key result of this work is that the DWM model in most cases coincides superiorly with the measurement results compared to the other engineering wake models commonly used in industry.

## 1. Introduction

When planing new wind farms, an accurate prediction of power output and turbine loads is highly relevant. For this reason, it is necessary to predict wind speed and turbulence inside a wind farm as exactly as possible in an acceptable period of time. Simple analytical wake models, which define the wind speed deficit and/or the turbulence in the wake, are used in industrial applications. Analytical turbulence models, such as the Frandsen model, define the total turbulence, which consists of the square sum of the ambient turbulence and an added induced turbulence due to the wind farm itself [1]. This total turbulence is valid inside a calculated wake cone angle and used in a site specific load calculation procedure. Another analytical model, which has similar low computational costs as the Frandsen model, is the Larsen model. In addition to the description of the total turbulence Larsen provides a definition of the wind speed deficit in the wake, which is used in this work [2]. The mentioned Jensen model also defines a description of the wind speed deficit [3].

Apart from these models some further simple analytical models exist to describe the wind speed deficit or the added turbulence. For example Frandsen presented in [4] an additional method to calculate the wind speed deficit. This model is primarily developed for the calculation of evenly distributed rows of offshore wind turbines. Further models for the estimation of the wind speed deficit or turbulences in the wake can be found in [5] or [6].



Another possibility and probably a more accurate method to define the wind turbine wake is a CFD (Computational Fluid Dynamic) simulation. Numerical simulation techniques have high computational cost and is nowadays still too computationally expensive and complex for the application in standard site specific load calculations. A method that ranks between CFD simulations and simple analytical engineering models is the aforementioned DWM model, which will be part of the IEC 61400-1 Ed. 4 [7]. The DWM model has significantly lower computational costs than a CFD simulation and is closer to the physics than purely analytical models, which is why it seems to be promising for industrial applications and could be an alternative to the commonly used models. A more detailed explanation of this model and the mentioned engineering models is given in the next section.

## 2. Description of wake models

### 2.1. Frandsen-model

The Frandsen model is a frequently used turbulence model, which is defined in the IEC 61400-1 Ed.3 [8]. The model defines the total turbulence  $I_t$  as follows [8]:

$$I_t = \sqrt{\frac{1}{\left(1,5 + 0,8 \frac{x/d}{\sqrt{c_t}}\right)^2} + I_0^2} \quad (1)$$

with  $I_0$  the ambient turbulence intensity,  $c_t$  the thrust coefficient,  $d$  the turbine diameter, and  $x$  the downstream distance. The total turbulence is assumed to be constant inside the wake cone, which is described by following equation [1]:

$$\Theta_w = \frac{1}{2} \left( \frac{180}{\pi} \cdot \tan^{-1} \left( \frac{1}{x/d} \right) + 10^\circ \right) \quad (2)$$

### 2.2. Larsen-model

Another engineering model is the G. C. Larsen model, which is introduced in [2] and recalibrated in [9]. The wind speed deficit and the wake radius  $R_w$  can be calculated depending on the rotor area  $A$ , the radial hub distance  $r$ , and the downstream distance  $x$  as follows [2]:

$$U_w = U_0 - \frac{U_0}{9} (c_t A x^{-2})^{\frac{1}{3}} \left( r^{\frac{3}{2}} (3c_1^2 c_t A x)^{-\frac{1}{2}} - \left( \frac{35}{2\pi} \right)^{\frac{3}{10}} (3c_1^2)^{-\frac{1}{5}} \right)^2 \quad (3)$$

$$R_w = \left( \frac{35}{2\pi} \right)^{\frac{1}{5}} (3c_1^2)^{\frac{1}{5}} (c_t A x)^{\frac{1}{3}} \quad (4)$$

The variable  $c_1$  is calculated according to the recalibrated version in [9].

Besides the definition of the wind speed deficit a method for the calculation of a rotor averaged wind speed is defined in [9], which is also used in this work. Two possibilities for calculating the mean wind speed reduction are given. The first one is a linear geometric averaging. The second one is based on a quadratic averaging approach, which seems to be more promising when looking at turbine loads. Therefore, the quadratic approach is used.

The total turbulence  $I_t$  and the added wake turbulence  $I_w$  are calculated with following equations [10]:

$$I_t = \sqrt{I_0^2 + I_w^2} \quad (5)$$

$$I_w = 0,29 \left( \frac{x}{d} \right)^{-\frac{1}{3}} \sqrt{1 - \sqrt{1 - c_t}} \quad (6)$$

### 2.3. Jensen-model

Another simple analytical model for calculating the wake wind speed deficit is the N.O. Jensen model, which is described in [3] and further developed in [11]. The model delivers the following equation to calculate wind speed inside the wake [11]:

$$U_w = \left( 1 - \frac{1 - \sqrt{1 - c_t}}{(1 + 2k\frac{x}{d})^2} \right) U_0 \quad (7)$$

with  $k$  being the decay constant of 0.075. The wake width is determined by the expression  $1 + 2k\frac{x}{d}$ .

### 2.4. DWM-model

The above mentioned models are compared to the dynamic wake meandering (DWM) model, which is based on the assumption that the wake behaves as a passive tracer in the turbulent wind field whereby the movement of the passive structure, i.e. the wake deficit, is driven by large turbulence scales [12], [13]. The DWM model can be divided into three parts. Figure 1 illustrates the main components of the model as well as input and output variables.

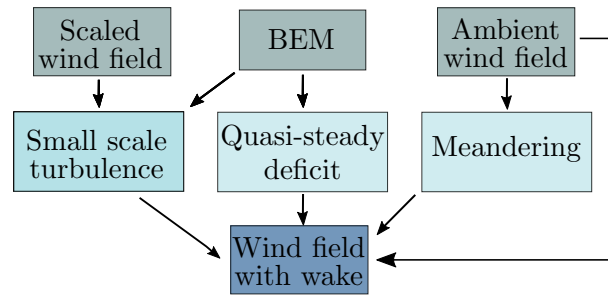


Figure 1: Components of the dynamic wake meandering model

#### 2.4.1. Quasi-steady wake deficit

The first part is the quasi-steady wake deficit, which is defined in the meandering frame of reference. This part consists of a formulation of the initial deficit emitted by the turbine upstream and the expansion of the deficit downstream [14]. In this study different methods to calculate the quasi-steady wake deficit are analysed. All of them have in common that the initial deficit is calculated based on the blade element momentum (BEM) theory respectively the axial induction factor derived from it. The expansion of the wind speed deficit downstream is computed based on the thin shear layer approximation of the Navier-Stokes equations in its axisymmetric form, which can be described depending on the wind speed in axial and radial direction  $U$  and  $V_r$  (see equations 8 and 9). This method is based on the work of J.F. Ainslie [15] and outlined in [12].

$$U \frac{\partial U}{\partial x} + V_r \frac{\partial U}{\partial r} = \frac{1}{r} \frac{\partial}{\partial r} \left( \nu_T r \frac{\partial U}{\partial r} \right) \quad (8)$$

$$\frac{1}{r} \frac{\partial}{\partial r} (r V_r) + \frac{\partial U}{\partial x} = 0 \quad (9)$$

The initial deficit serves as a boundary condition when solving the Navier-Stokes equations. Pressure terms in the thin shear layer equations are neglected. The error, which is made by this assumption is compensated by taking the wind speed deficit at two rotor diameters downstream (beginning of the far wake area) as a boundary condition at the position directly after the rotor.

The thin shear layer equations are solved by a finite differences method. An eddy viscosity ( $\nu_T$ ) closure approach is used for solving. As already mentioned, different methods for the computation of the quasi-steady wake deficit in the DWM model are validated. The methods differ in the calculation of the initial deficit and the eddy viscosity formulation. The three analysed methods are given as follows:

#### 1. DWM-IEC:

In the draft of the IEC 61400-1 Ed.4 standard the calculation of the initial deficit (wake wind speed  $U_w$  and wake radius  $R_w$ ) is based on the rotor averaged induction factor and is described as follows [7]:

$$U_w = U_0 (1 - 2\bar{\alpha}) \quad (10)$$

$$R_w = 2R (1 - 0.45\bar{\alpha}^2) \sqrt{\frac{1+m}{8}} \quad (11)$$

with

$$m = \frac{1}{\sqrt{1 - c_t}} \quad (12)$$

$\bar{\alpha}$ : rotor averaged induction factor

The eddy viscosity is defined as [7]:

$$\frac{\nu_T}{U_0 R} = 0.023 F_1(\tilde{x}) I_0^{0,3} + 0.016 F_2(\tilde{x}) \frac{R_w(\tilde{x})}{2R} \left( 1 - \frac{U_{min}(\tilde{x})}{U_0} \right) \quad (13)$$

with

$R$ : rotor radius

$U_{min}$ : wind speed minimum

$\tilde{x}$ : axial distance normalized by the rotor radius

$F_1$  and  $F_2$ : filter functions defined in [7]

#### 2. DWM-Madsen:

In [16] following formulae are given to calculate the wind speed deficit and the wake radius at the border between the near and far wake region with respect to the radial positions  $r_{w,i}$  and  $r_{w,i+1}$ :

$$U_w((r_{w,i+1} + r_{w,i})/2) = U_0(1 - 2\alpha_i) \quad (14)$$

$$r_{w,i+1} = \sqrt{\frac{1 - \alpha_i}{1 - 2\alpha_i} (r_{i+1}^2 - r_i^2) + r_{w,i}^2} f_w \quad (15)$$

with

$$f_w = 1 - 0.45\bar{\alpha}^2 \quad (16)$$

$r_{w,i}$ : wake radius at position  $i$

$\alpha_i$ : induction factor at position  $i$

$r_i$ : rotor radius at position  $i$

For the calculation of the eddy viscosity the following equations are declared in [16] and further developed in [17]:

$$\frac{\nu_T}{U_0 R} = 0.008 F_2(\tilde{x}) \frac{R_w(\tilde{x})}{R} \left( 1 - \frac{U_{min}(\tilde{x})}{U_0} \right) + 0.1 F_1(\tilde{x}) F_0 I_0 \quad (17)$$

with

$F_0$ : nonlinear coupling function defined in [17]

### 3. DWM-Keck:

The last method defines the initial deficit by the following equations [18]:

$$U_w(r_{w,i}) = U_0 (1 - (1 + 1.1) \alpha_i) \quad (18)$$

$$r_{w,i} = r_i \sqrt{\frac{1 - \bar{\alpha}}{1 - (1 + 0.98) \bar{\alpha}}} \quad (19)$$

In [18] the final and recommended version the eddy viscosity is defined as follows:

$$\nu_T = 0.587F_1(\tilde{x})u^*l^* + 0.0178F_2(\tilde{x}) \max\left(l^{*2} \left| \frac{\partial U(\tilde{x})}{\partial r} \right|, l^* (1 - U_{min}(\tilde{x}))\right) \quad (20)$$

The definition in (20) differs from the other models by using the velocity and length scales ( $u^*$  and  $l^*$ ) of the atmospheric turbulence.  $u^*$  and  $l^*$  imply the velocity and length scales of the ambient turbulence fraction, which corresponds to the wake evolution. It can be assumed that the mixing length  $l^*$  is equal to half of the wake width [18]. In this work the part of the considered velocity and length scales of the ambient turbulence are simplified by using the ambient turbulence intensity. Therefore, the atmospheric stability is not considered in this implementation, as it is proposed in [19], and equation (20) reads as changes to

$$\frac{\nu_T}{U_0 R} = 0.0914F_1(\tilde{x})I_0 + 0.0216F_2(\tilde{x}) \max\left(\frac{R_w(\tilde{x})^2}{RU_0} \left| \frac{\partial U(\tilde{x})}{\partial r} \right|, \frac{R_w(\tilde{x})}{R} \left(1 - \frac{U_{min}(\tilde{x})}{U_0}\right)\right) \quad (21)$$

The constants were taken from the results of the least-square recalibration in [18].

#### 2.4.2. Meandering

The second part of the model is the meandering itself. The meandering is based on the large turbulence scales of the ambient turbulent wind field and can be calculated from the low pass filtered ambient wind field, which is generated with a Kaimal spectrum. The cut-off frequency is specified by the wind speed and the rotor diameter as follows [17]:

$$f_c = \frac{U}{4R} \quad (22)$$

The lateral  $y(t)$  and vertical  $z(t)$  position of the wake deficits depends on the wind speed fluctuations at hub height in horizontal and vertical direction (see equation (23) and (24)) [12]. The usage of the filtered wind speed at hub height is a simplification, which is made here.

$$\frac{dy(t)}{dt} = v(t) \quad (23)$$

$$\frac{dz(t)}{dt} = w(t) \quad (24)$$

#### 2.4.3. Small scale turbulence

The last part of the DWM model is the description of the small scale turbulence, which is generated through the wake shear itself as well as tip and root vortices at the blades. This turbulence part is calculated with a scaled homogeneous turbulent windfield generated with the Kaimal spectrum. The method and scaling factor is calculated according to [7]. Originally, the added or small scaled turbulence field is defined in the meandering frame of references. In this work only the scaling function meanders which leads to slight differences compared to the original model, which however can be neglected for the outlined validation.

### 3. Wind farms

The presented results are based on measurements from the ECN test site EWTW (ECN Wind turbine test site Wieringermeer). The wind farm consists of five Nordex turbines (N80/2.5). In [20] a more detailed explanation of the wind farm conditions and the load measurement are given. A met mast is located in a distance of 280 m respectively 200 m from the observed turbines, so that two different wake situations with different distances could be analysed. The measured wind speeds at hub height from the mast are used to determine the wake situation downstream of the wind turbine. Additionally, load measurements at one turbine could be used for validation purposes, so that loads could be measured under wake conditions. The second analysed wind farm is the wind farm Høvsøre which is located on the Danish west coast. During the measurements the wind farm consists of four different wind turbines and a met mast. Turbine data from a Nordex turbine (N100/3.3) are used for validation purposes. The measured wind speeds from the mast are used to determine wake situation 250 m downstream.

### 4. Results

This section compares measurements from the described wind farms with simulated wind speeds, power and loads. Figure 2 and Figure 3 depict the measured and simulated wind speeds and turbulence intensities over the wind direction in Høvsøre. Error bars of plus and minus one standard deviation of the measurements are also shown. Simulations with variations of the DWM-Model were done. In this case a wind direction of  $0^\circ$  means that the met mast is in full wake of the wind turbine. The measured wind speeds are normalized by the ambient wind speed of 10 m/s. Thereby, it should be noticed that the only differences in the DWM-Models are the calculation of the initial deficit (ID) and the eddy viscosity (EV) as explained before. Three DWM-simulations were performed with the eddy viscosity calculation based on the IEC guideline. In addition, two simulations were computed with the same initial deficit method and variations of the eddy viscosity method. Furthermore, results from the Keck-Model with a consistent calculation of initial deficit and eddy viscosity are illustrated. The eddy viscosity calculated by the IEC guideline delivers the same results as the here called DWM-Madsen method. Because of that the blue dashed curve is covered by the ID-Madsen/EV-Madsen curve. The individual variation of the initial deficit and eddy viscosity method clearly shows the impact of the single methods themselves. The simulations with constant eddy viscosity and variation of the initial deficit differ only slightly, while in contrast, the ID-Madsen/EV-Madsen and ID-Madsen/EV-Keck curves differ substantially. Especially the turbulence intensity varies clearly at partial wake conditions.

When looking at the self-consistent calculation methods (ID-IEC/EV-IEC, ID-Madsen/EV-Madsen and ID-Keck/EV-Keck) the Keck-Model achieves the best matching with the measurement results. The other methods deliver higher turbulence intensities than measured, particularly at partial wake conditions. The measured values are filtered by the ambient turbulence intensity of 8%. The ambient turbulence intensity is determined by the nacelle anemometer measurements at the turbine. When looking at the edges of the measured turbulence intensity curve the ambient turbulence intensity at the met mast seems a bit higher as the one determined by the nacelle anemometer. Figure 4 and 5 depict the simulated power and the damage equivalent loads (DELs) of the flapwise blade root bending moment with different DWM-Model variations. In these simulations it is assumed that a fictive turbine is located at the position of the met mast. The turbine type of this fictive turbine is the same as the wake generating turbine (N100/3.3). The simulations were done with ALASKA/WIND, which is an aeroelastic load simulation tool. The simulated power and flapwise moment curves show that there is a clear correlation between power and wind speed respectively flapwise moment and turbulence intensity. Thus, it can be stated that qualitative differences between the methods in power output and loads can already be determined by the wind speed deficit and turbulence

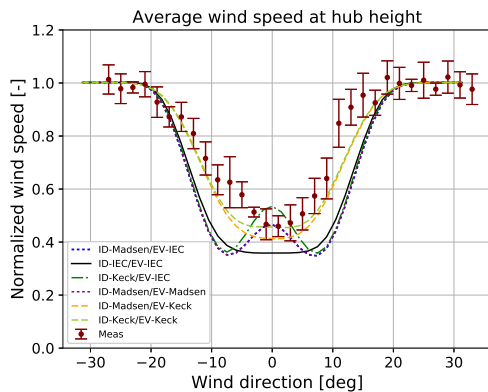


Figure 2: Simulated and measured wind speeds at 250 m downstream at Høvsøre

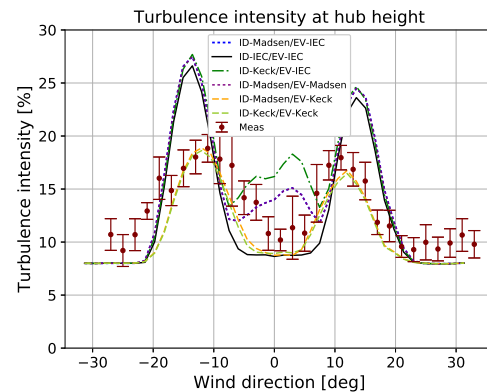


Figure 3: Simulated and measured turbulences at 250 m downstream at Høvsøre

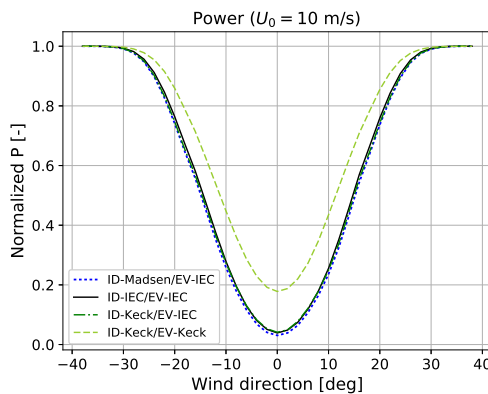


Figure 4: Simulated power at 250 m downstream

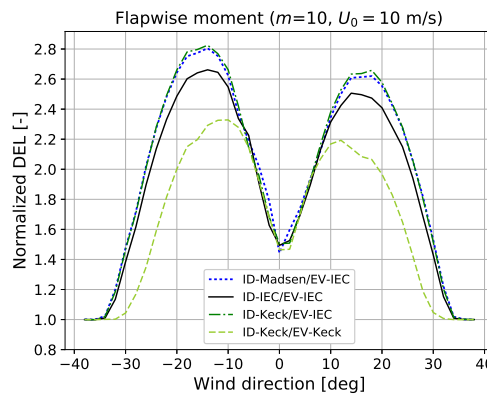


Figure 5: Simulated DELs of the flapwise blade root bending moment at 250 m downstream

intensity curves themselves. Thereby, it can be proved that the impact of different models on loads and power output is not negligible.

Figure 6 depicts measured and simulated wind speeds over different wind directions at the EWTW. The corresponding turbulence intensities are illustrated in figure 7. The measured wind speed is normalized by the ambient wind speed of 9 m/s, which is determined by the nacelle anemometer measurements at the turbine. The measured wake conditions were calculated with five different models in case of the turbulence intensity and four models in case of the wind speed. Only the consistent DWM-Models were used in this case and compared to the analytical Frandsen, Larsen and Jensen model. For Frandsen's and Larsen's model, the wake turbulence is assumed to be constant inside the wake. The Jensen model assumes a constant wind speed inside the wake. This leads to the rectangular shape of the respective curves. The figure also shows that the best matching with measured values can be achieved with the DWM-Keck model. This applies for the wind speed deficit as well as turbulence intensity. The Larsen and the Jensen model underestimate the wind speed deficit while the other DWM model variations overestimate the wind speed deficit. When looking at the turbulence intensity it can be seen that the Frandsen model and the DWM-Madsen model as well as the DWM-IEC model deliver significantly higher turbulences at partial wake conditions than measured. The overestimation

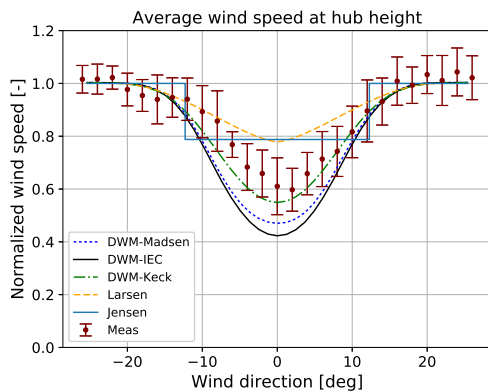


Figure 6: Simulated and measured wind speeds at 280 m downstream at the EWTW

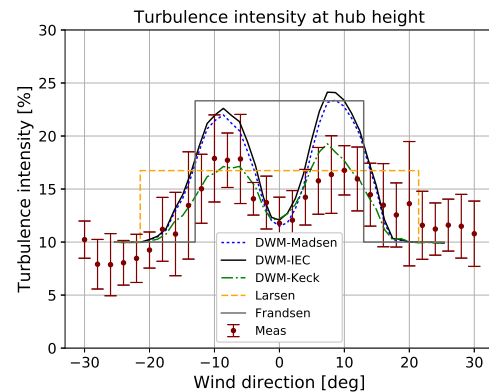


Figure 7: Simulated and measured turbulences at 280 m downstream at the EWTW

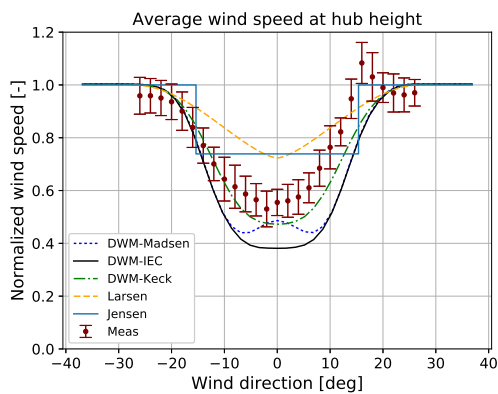


Figure 8: Simulated and measured wind speeds at 200 m downstream at the EWTW

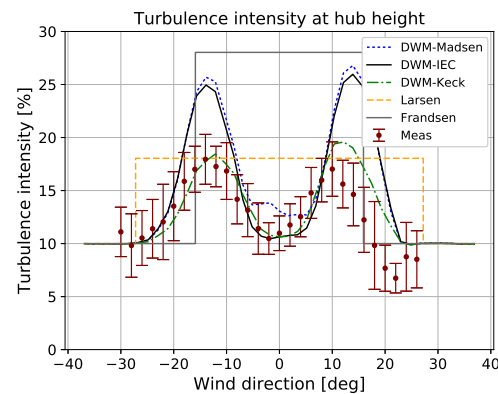


Figure 9: Simulated and measured turbulences at 200 m downstream at the EWTW

at partial wake conditions is even more significant at 200 m downstream (see figure 9). The wind speed deficit simulated and measured at 200 m downstream is illustrated in 8. At 200 m downstream the wind speed deficit is more pronounced and less degraded than at 280 m.

Figure 10 depicts the measured and simulated power with the Larsen model and the Keck-DWM model over the wind direction at 9 m/s. The simulations were done with FLEX5. The Larsen model uses a quadratic averaged wind speed over the rotor swept area as proposed in [9] and mentioned in the previous section. Figure 10 shows that the Larsen model underestimates and the DWM model slightly overestimates the power deficit. This could already be observed at the wind speed deficit. Figure 11 depicts the DEL of the tower bottom bending moment. In this case a good accordance with measured values can be achieved with the DWM-Keck model and the Larsen model. The Frandsen model mostly overestimates the loads. The shown numbers at each curve represent the DEL over all wind directions. The mean DELs over the presented wind directions are calculated with respect to the Wöhler coefficient and an even wind direction distribution. The mean DEL calculated by the Larsen model (1.43) is the nearest to the measured one (1.29). Figure 12 and 13 illustrate the DEL of the edgewise and flapwise blade root bending moment. The influence of the wake on the edgewise moment is rather low as expected. Because of that, a significant difference between the models cannot be stated for this sensor. When looking at the flapwise moment the difference between the models is much higher.

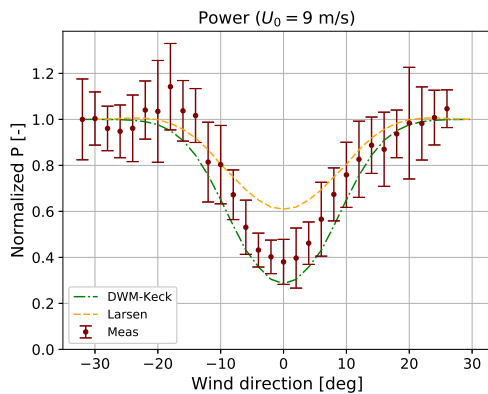


Figure 10: Simulated and measured power at 305 m downstream at the EWTW

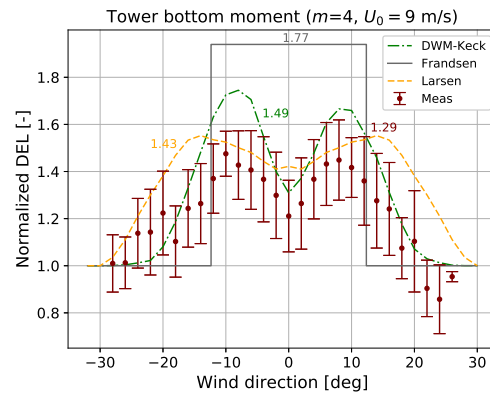


Figure 11: Simulated and measured DELs of the tower bottom bending moment at 305 m downstream at the EWTW

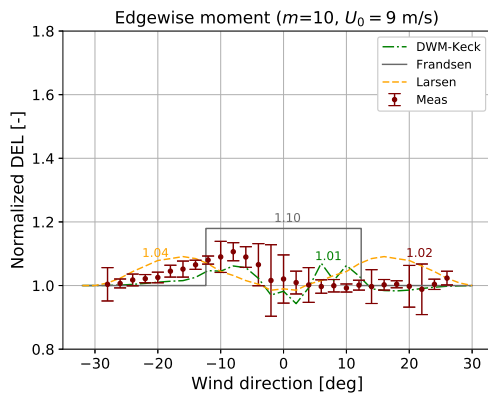


Figure 12: Simulated and measured DELs of the edgewise blade root bending moment at 305 m downstream at the EWTW

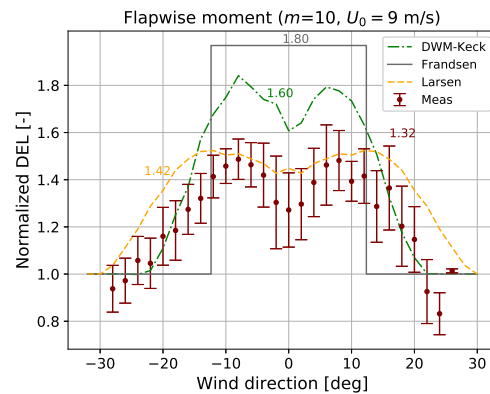


Figure 13: Simulated and measured DELs of the flapwise blade root bending moment at 305 m downstream at the EWTW

The DWM model as well as the Frandsen model overestimate the flapwise moment at partial wake conditions in most instances. The Larsen model coincides better with the measurements.

## 5. Conclusion

This study addresses the validation of the DWM model with different calculation methods for the quasi-steady wake deficit and compares it to commonly used models. In general, it could be said that the Frandsen model mainly delivers too high loads in wake situations, whereas the DWM model coincides better with measured values. However, the calculation method for the quasi-steady deficit naturally has a huge impact on the overall result of the DWM-Model. It is also worth mentioning that the analytical Larsen model with a rotor averaged wind speed provides a better match with the measured values than the Frandsen model while still being conservative. Nevertheless, the wind speed and power deficit are less well predicted by this model. Furthermore, the influences of the calculation methods of the initial deficit and the eddy viscosity method were analysed. While the influence of different approaches for the determination of the initial deficit is rather small, the impact of the used equation for the eddy viscosity is in fact more significant. The different models were used in a load calculation software to quantify the impact of the different models on turbine loads and power output and to clarify

that the influence of the different models on loads and power generation proves to be by no means negligible.

### Acknowledgments

This paper was developed within the project NEW 4.0 (North German Energy Transition 4.0), which is partly funded by the Federal Ministry for Economic Affairs and Energy (BMWi). In addition, special thanks go to ECN (Energy research Centre of the Netherlands) for providing the measurement data. The measurements were carried out in the framework of the LAWINE project funded by TKI Wind op Zee.

### References

- [1] Frandsen S 2007 *Turbulence and turbulence-generated structural loading in wind turbine clusters* Ph.D. thesis Technical University of Denmark
- [2] Larsen G C 1988 A simple wake calculation procedure Tech. Rep. Risø-M-2760 Risø National Laboratory
- [3] Jensen N O 1983 A note on wind generator interaction Tech. Rep. Risø-M-2411 Risø National Laboratory
- [4] Frandsen S, Barthelmie R, Pryor S, Rathmann O, Larsen S, Højstrup J and Thøgersen M 2006 *Wind Energy* **9**(1-2) pp 39–53
- [5] Bastankhah M and Port-Agel F 2014 *Renewable Energy* **70**(Januar 2014) pp 116–123
- [6] Crespo A and Herna J 1996 *J. Wind Eng. Ind. Aerodyn.* **61**(1) pp 71–85
- [7] 2016 IEC 61400-1 Ed. 4, CDV: Wind energy generation systems - Part 1: Design requirements Guideline International Electrotechnical Commission (IEC)
- [8] 2010 IEC 61400-1 Ed. 3, A1: Wind turbines - Part 1: Design requirements Guideline International Electrotechnical Commission (IEC)
- [9] Larsen G C 2009 A simple stationary semi-analytical wake model Tech. Rep. Risø-R-1713(EN) Risø National Laboratory
- [10] 1998 European wind turbine standards II Guideline ECN Solar & Wind Energy
- [11] Katić I, Højstrup J and Jensen N O 1987 A simple model for cluster efficiency *EWEC'86. Proceedings. Vol. 1* ed Palz W and Sesto E (Rome: A. Raguzzi) pp 407–410
- [12] 2007 Dynamic wake meandering modeling Tech. Rep. Risø-R-1607(EN) Risø National Laboratory
- [13] Larsen G C, Madsen H A, Thomsen K and Larsen T J 2008 *Wind Energy* **11**(4) pp 377–395
- [14] Larsen G C, Madsen H A, Larsen T J and Troldborg N 2008 Wake modeling and simulation Tech. Rep. Risø-R-1653(EN) Risø National Laboratory for Sustainable Energy
- [15] Ainslie J F *J. Wind Eng. Ind. Aerodyn.* **27** pp 213–224
- [16] Madsen H A, Larsen G C, Larsen T J and Troldborg N 2010 *J. Sol. Energy Eng.* **132**(4) 041014
- [17] Larsen T J, Madsen H A, Larsen G C and Hansen K S 2013 *Wind Energy* **16**(4) pp 605–624
- [18] Keck R E, Madsen H A, Larsen G C, Veldkamp D and Wedel-Heinen J 2013 *A consistent turbulence formulation for the dynamic wake meandering model in the atmospheric boundary layer* Ph.D. thesis Technical University of Denmark
- [19] Keck R E, de Maré M, Churchfield M J, Lee S, Larsen G and Madsen H A 2014 *Wind Energy* **17**(11) pp 1689–1710
- [20] Poodt M J S and Wouters D A J 2017 On the added benefits of ground-based LiDAR for wind turbine load measurements Tech. Rep. ECN-E-16-051 Energy research Centre of the Netherlands